ELSEVIER

Journal of Membrane Science 191 (2001) 179–187

journal of MEMBRANE SCIENCE

www.elsevier.com/locate/memsci

Ion size effects on the current efficiency of narrow charged pores

Javier Cervera, José A. Manzanares*, Salvador Mafé

Departament de Termodinàmica, Facultat de Física, Universitat de València, 46100 Burjassot, Spain

Received 27 July 2000; received in revised form 19 April 2001; accepted 19 April 2001

Abstract

The effects of ion size on the current efficiency (CE) of charged membranes with narrow pores are studied theoretically. The CE is a measure of the membrane permselectivity defined as the ratio between the counterion flux and the sum of the counterion and coion fluxes when an electric potential difference is applied between the two solutions bathing the membrane. It is studied here as a function of two relevant experimental parameters: the ratio between the ionic radius and the pore radius, and the ratio between the external salt concentration and the membrane fixed charge concentration. The ratio of the CE values corresponding to the point and finite size ions is also calculated as a function of the above two parameters. Ion size effects are introduced in the ionic diffusion coefficients (by means of the Renkin function) as well as in the ionic concentration profiles. It is shown that a significantly higher coion exclusion from the membrane and thus a higher CE is obtained for finite size ions compared to the case of point ions.

Keywords: Current efficiency; Ion size effects; Space charge model

1. Introduction

Ionic transport processes through artificial and biological membranes are usually studied on the basis of a physical model that simulates the membrane by an array of parallel charged cylindrical pores [1,2]. The membrane pores do not act simply as mechanical filters: they display also ionic selectivity due to the electrical charges bound to the pore surface.

The diffuse double layer theory can give a suitable description of the radial ion distribution in the pore only when the ionic concentrations are low enough. At high pore surface charge density and ionic concentrations, however, ion size effects need to be included in order to avoid unrealistic ion accumulation near charged surfaces [3–10]. These effects are crucial for the ion distribution in the vicinity of a planar charged surface immersed in an electrolyte solution [11–13], in the passive diffusion of ionic drugs across the paracellular pathway of cell monolayers simulating the intestinal mucosa where the effective pore radius is similar to that of the drug [14,15], and in determining the current efficiency (CE) of narrow membrane channels [16]. However, theoretical studies that quantify ion size effects on transport through porous media are lacking [8–10].

We aim at studying the effects of the finite ion size on the CE of narrow charged cylindrical pores. For the sake of simplicity, the external solutions are considered identical, thus avoiding the effects of a diffusion potential hindering those of the finite size of the ions. The CE is a measure of the membrane selectivity defined as the ratio between the counterion flux and the sum of the counterion and coion fluxes [17]. It is studied here as a function of two relevant experimental parameters: the ratio between the ionic radius and the pore radius, and the ratio between the

* Corresponding author.
E-mail address: manzanar@uv.es (J.A. Manzanares).

0376-7388/01/$ – see front matter
PII: S0376-7388(01)00466-5

external electrolyte concentration and the membrane fixed charge concentration. We have employed a generalized Poisson–Boltzmann (PB) equation that incorporates the ion size by means of the Bikerman equation [13]. The radial distributions of the electric potential and the ionic concentrations in the pore are obtained by solving the extended PB equation. Recent work has shown that mean field theories, like the one employed in this work, are in agreement with the results obtained by means of Brownian dynamics simulations up to a ratio of the pore radius to the Debye length around 3 [18]. This places a limit on the system parameters that can be used.

2. Formulation of the problem

Consider a negatively charged membrane separating two identical solutions of a 1:1 binary electrolyte at concentration c^{b}. The membrane is modeled as an array of parallel cylindrical pores with a surface charge density $\sigma < 0$ at the pore wall. The pore length is assumed to be much larger than its radius a, so that edge effects can be neglected. A schematic view of the pore model is shown in Fig. 1. Thermal equilibrium at temperature T and steady-state conditions are assumed.

Due to the applied electric potential difference between the two external solutions, an electric current density flows through the pores. The solution filling the pores has a positive electric charge density which compensates for the surface charge density σ at every axial position along the pore length. Thus, the current density is mostly transported by the cations and $|J_+| > |J_-|$, where J_+ and J_- are the fluxes of the cations and anions through the pores in the membrane–fixed reference frame. This property of charged membranes is characterized in terms of the CE, defined as [19,20]

$$\mathrm{CE} = \frac{|J_+|}{|J_+| + |J_-|}. \tag{1}$$

The aim of this study is to evaluate the effects of ion size on CE, which requires the calculation of the ion fluxes.

The presence of an electric charge density at the pores walls also implies that there is volume flow through the pores, even in the absence of an applied pressure difference between the external solutions. This flow arises from the electrical force that acts on the positively charged pore solution, and can be assumed to be laminar under most experimental conditions. Thus, we introduce $u(r)$ as the pore solution velocity along the pore axis, which is only a function of the radial position r.

The fluxes in Eq. (1) are obtained by integration over the pore cross-section

$$J_i = \int_0^{a_i^*} j_i 2\pi r \, \mathrm{d}r \tag{2}$$

of the axial components of the flux densities

$$j_i(r) = -\frac{D_i c_i(r)}{RT} \frac{\mathrm{d}\widetilde{\mu}_i(x)}{\mathrm{d}x} + c_i(r)\, u(r), \tag{3}$$

where c_i, D_i, $\widetilde{\mu}_i$ are the molar concentration, diffusion coefficient, and electrochemical potential of species i ($i = +, -$), respectively, and R is the gas constant. The ions are modeled as hard spheres with a central charge. Therefore, the upper integration limit in Eq. (2) is defined as the position of closest approach of the charges to the pore wall, $a_i^* = a - a_i$, where a_i is the ion radius and a is the pore radius. (Note that the continuity equations for ionic fluxes and volume flow have been implicitly used to determine the functional dependence of the magnitudes in Eq. (3)).

To account for the ion size effects in the diffusion process, the diffusion coefficient is modified by means

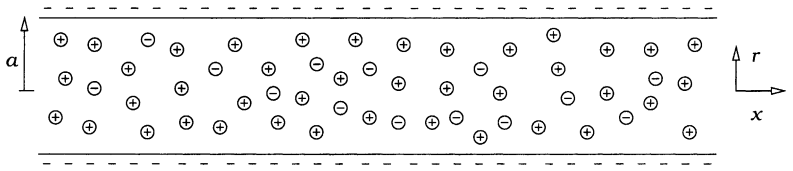

Fig. 1. Schematic view of a section of the membrane pore.

of the Renkin function [21]

$$\frac{D_i}{D_i^0} = \left(1 - \frac{a_i}{a}\right)^2 \times \left[1 - 2.104\left(\frac{a_i}{a}\right) + 2.09\left(\frac{a_i}{a}\right)^3 - 0.95\left(\frac{a_i}{a}\right)^5\right], \tag{4}$$

where D_i^0 is the ionic diffusion coefficient in free solvent. Renkin equation is valid only for $a_i/a \leq 0.4$.

Owing to the non-penetrability of the pore walls, it is reasonable to assume that the radial component of the flux densities vanishes, which is equivalent to stating that the electrochemical potential [22]

$$\widetilde{\mu}_i(x) = \mu_i^0 + RT\ln c_i(r) + z_i F\phi(r,x) + v_i p(r), \quad i = +, - \tag{5}$$

is independent of the radial position. In Eq. (5), μ_i^0, z_i, and v_i are the standard chemical potential, the charge number, and the partial molar volume of species i, p the pressure, F the Faraday constant, and ϕ the electric potential. Since Eq. (3) implies that $\widetilde{\mu}_i(x)$ is a linear function of x, and c_i is independent of x, we see from Eq. (5) that the electric potential can be written as the sum of two terms, one linear in x and the other one depending on r, $\phi(r,x) = V(x) + \psi(r)$. Eq. (3) takes then the form

$$j_i = -z_i D_i c_i \frac{F}{RT}\frac{\mathrm{d}V}{\mathrm{d}x} + c_i u. \tag{6}$$

The solution velocity u is given by the axial component of the Navier–Stokes equation

$$\eta\frac{1}{r}\frac{\mathrm{d}}{\mathrm{d}r}\left(r\frac{\mathrm{d}u}{\mathrm{d}r}\right) = \rho_\mathrm{e}\frac{\mathrm{d}V}{\mathrm{d}x}, \tag{7}$$

where η is the dynamic viscosity and $\rho_\mathrm{e} = F\sum_i z_i c_i$ is the volume electrical charge density in the pore solution. By eliminating ρ_e between Eq. (7) and the Poisson equation

$$\frac{1}{r}\frac{\mathrm{d}}{\mathrm{d}r}\left(r\frac{\mathrm{d}\psi}{\mathrm{d}r}\right) = -\frac{\rho_\mathrm{e}}{\varepsilon}, \tag{8}$$

where ε is the dielectric permittivity of the solution, and integrating from $r = 0$ to r, the following relation is easily obtained:

$$\eta\frac{\mathrm{d}u}{\mathrm{d}r} = -\varepsilon\frac{\mathrm{d}V}{\mathrm{d}x}\frac{\mathrm{d}\psi}{\mathrm{d}r}. \tag{9}$$

Therefore, the solution velocity is related to the electric potential by

$$u(r) = \frac{\varepsilon}{\eta}\frac{\mathrm{d}V}{\mathrm{d}x}[\psi(a) - \psi(r)], \tag{10}$$

where the non-slip boundary condition $u(a) = 0$ has been used.

The radial distribution of $\psi(r)$ is obtained by numerical integration of Eq. (8) subject to the boundary conditions

$$\left.\frac{\mathrm{d}\psi}{\mathrm{d}r}\right|_{r=0} = 0, \tag{11}$$

and [23]

$$\left.\frac{\mathrm{d}\psi}{\mathrm{d}r}\right|_{r=a_i^*} = \frac{\sigma}{\varepsilon}\frac{a}{a - a_i}. \tag{12}$$

Eq. (12) takes into account the fact that the ions have been modeled as hard spheres with a central charge. The electric potential gradient at the point of closest approach of the charges must then be higher in the finite ion size case than in the point ion case so that electroneutrality in the pore cross-section is maintained. To integrate Poisson equation, the relation between ρ_e and ψ has to be deduced from the radial component of the Navier–Stokes equation

$$\frac{\mathrm{d}p}{\mathrm{d}r} + \rho_\mathrm{e}\frac{\mathrm{d}\psi}{\mathrm{d}r} = 0, \tag{13}$$

and the equilibrium condition along the radial direction

$$\frac{\mathrm{d}c_i}{\mathrm{d}r} + z_i c_i\frac{F}{RT}\frac{\mathrm{d}\psi}{\mathrm{d}r} + \frac{c_i v}{RT}\frac{\mathrm{d}p}{\mathrm{d}r} = 0, \quad i = +, -, \tag{14}$$

where, for the sake of simplicity, the partial molar volumes of cations and anions have been assumed to be equal, $v_+ = v_- = v$. Summing Eq. (14) over species i, it is easy to eliminate either $\mathrm{d}p/\mathrm{d}r$ or $\mathrm{d}\psi/\mathrm{d}r$ and obtain the equations

$$c_i(r) = \frac{1 - v\sum_i c_i(r)}{1 - v\sum_i c_i(0)}c_i(0) + \exp\left\{-z_i\frac{F}{RT}[\psi(r) - \psi(0)]\right\}, \tag{15}$$

and

$$p(r) = p(0) - \frac{RT}{v}\ln\left(\frac{1 - v\sum_i c_i(r)}{1 - v\sum_i c_i(0)}\right), \tag{16}$$

which are generalizations of the Boltzmann and Van't Hoff osmotic pressure equations, respectively. Eq. (15) is known as the Bikerman equation [13]. To apply it, the values of the ionic concentrations and the electric potential in the pore center must be estimated from the corresponding values in the external solutions. If the current flow is not high, it can be assumed that the concentration and electric potential values in the pore center are those corresponding to the distribution equilibrium [24]

$$c_i(0) = \frac{1 - v\sum_i c_i(0)}{1 - 2vc^{\mathrm{b}}} c^{\mathrm{b}} \exp\left\{-z_i \frac{F}{RT}[\psi(0) - \psi^{\mathrm{b}}]\right\}, \tag{17}$$

and

$$p(0) = p^{\mathrm{b}} - \frac{RT}{v} \ln\left(\frac{1 - v\sum_i c_i(0)}{1 - 2vc^{\mathrm{b}}}\right), \tag{18}$$

where the superscript 'b' makes reference to the external solution values.

The numerical procedure that has been used to solve the extended PB equation is the shooting method [25]. A free parameter, $\psi(0) - \psi^{\mathrm{b}}$, needs to be varied until the two boundary conditions, Eqs. (11) and (12), are satisfied. The shooting method uses the same procedure employed to obtain the zeros of a function. In this case, the independent variable is the free parameter and the values of the "function" are obtained from the difference between Eq. (12) and the gradient of the electric potential at $r = a^*$ calculated numerically. To obtain the latter, the boundary condition at $r = 0$ and the value initially guessed for $\psi(0) - \psi^{\mathrm{b}}$ are used to integrate numerically the Poisson equation by means of a fourth order Runge–Kutta method. Once we obtain a positive and a negative value of the above "function", the search of the zero of the function can be done using iteratively the bisection or a Regula–Falsi method to the desired accuracy.

3. Results and discussion

The following results have been obtained considering a partial molar volume of the ions $v = 160\,\mathrm{cm^3\,mol^{-1}}$. Since the electrolyte solution has been modeled as a gas of hard spheres, the free volume accessible to the ions is reduced by the volume they occupy. Using this reduction of free volume, it can be shown from statistical mechanics that the value of the partial molar volume chosen is equivalent to an ionic radius of 0.2 nm [12]. The ionic radius corresponds to the hydrated species, since these are the species that exist in solution. The charge density at the pore wall is $\sigma = -4\,\mu\mathrm{C\,cm^{-2}}$, which amounts to a distance between charges of ca. 2 nm. Other parameters are $T = 300\,\mathrm{K}$, $\eta = 1\,\mathrm{mPa\,s}$, and $\varepsilon = 80\varepsilon_0$ where ε_0 is the vacuum permittivity. For the diffusion coefficients the Stokes–Einstein equation has been employed, $D_+^0 = D_-^0 = kT/6\pi\eta a_i$, where k is the Boltzmann constant. The results are discussed in terms of the ratio between ion and pore radii, a_i/a, and the ratio between the external solution concentration c^{b} and $X \equiv \sum_i z_i \langle c_i \rangle$, where $\langle c_i \rangle$ is the average concentration of species i in the pore solution. The fixed charge concentration X is related to the surface charge density σ on the pore wall by the condition of overall electroneutrality in the pore cross-section

$$X = -\frac{2a\sigma}{F(a_i^*)^2}. \tag{19}$$

Fig. 2 shows the ionic concentration profiles for the case $a_i/a = 0.15$ and $c^{\mathrm{b}}/X = 0.5$ or equivalently,

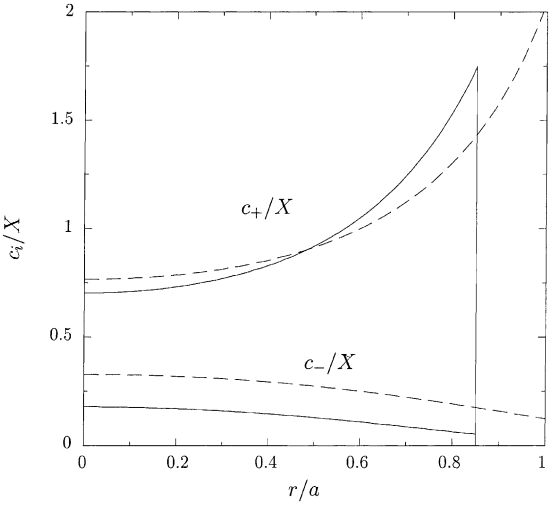

Fig. 2. Counterion (+) and coion (−) concentration profiles (normalized to the membrane fixed charge concentration X) inside the pore for $a_i/a = 0.15$ and $c^{\mathrm{b}}/X = 0.5$. Solid and dashed lines correspond to finite size and point ions, respectively. Note that for finite size ions, the upper limit of the radial variable is $a^* = a - a_i = 0.85a$.

$a \approx 1.3\,\text{nm}$, $c^{\text{b}} \approx 0.4\,\text{M}$, and $X \approx 0.8\,\text{M}$, the latter being a typical value for ion-exchange membranes [16,24]. The above values were chosen to emphasize the effects due to finite size of the ions while being within the range of validity of the mean field theory employed.

To better understand the effects due to the finite size of the ions in Fig. 2, consider first the point ions case, whose magnitudes are marked with the superscript '0' henceforth. The sum of the ionic concentrations in the pore solution is higher than that of the external solutions due to the existence of an electrical charge on the pore wall that need to be compensated by the ions in solution. This can be seen by setting $v = 0$ in Eq. (17) and calculating the total of species concentration as

$$c_+^0 + c_-^0 = 2c^{\text{b}} \cosh[\psi(0) - \psi^{\text{b}}], \tag{20}$$

which is higher than $2c^{\text{b}}$ since $\cosh[\psi(0) - \psi^{\text{b}}] \geq 1$. The boundary conditions, Eqs. (11) and (12), impose that the absolute values of both ψ and $\mathrm{d}\psi/\mathrm{d}r$ increase with r. Therefore, an increase of $c_+^0 + c_-^0$ is expected following that of $|\psi|$.

Ion size effects are introduced by means of the term in the electrochemical potential that accounts for the mechanical work. The species tend to move to regions where the value of its electrochemical potential is lower and, therefore, towards regions of lower pressure. If, as in the case of point ions, the sum of the ionic concentrations in the pore center is calculated, then

$$c_+(0) + c_-(0) = \frac{2c^{\text{b}} \cosh[\psi(0) - \psi^{\text{b}}]}{1 + 2vc^{\text{b}}\{\cosh[\psi(0) - \psi^{\text{b}}] - 1\}}, \tag{21}$$

and we see again that $c_+(0) + c_-(0) \geq 2c^{\text{b}}$. This result implies by Eq. (18) that the pressure at the pore center is higher than that of the external solutions. Therefore, a first consequence is that the finite size ions try to avoid entering the membrane pores. The equilibrium distribution assumed between the pore center and the external solution described by Eqs. (17) and (18) also implies that

$$c_+(0)c_-(0) = (c^{\text{b}})^2 \exp\left\{-\frac{2[p(0) - p^{\text{b}}]v}{RT}\right\}, \tag{22}$$

which leads to the relation $c_+(0)c_-(0) \leq (c^{\text{b}})^2$, where the equality $c_+(0)c_-(0) = (c^{\text{b}})^2$ corresponds to the point ions case. Applying the same reasoning to Eqs. (15) and (16) we obtain

$$c_+(r)c_-(r) \leq c_+(0)c_-(0) \leq (c^{\text{b}})^2, \tag{23}$$

where the equality corresponds to the limiting case of point ions. The average ionic concentrations $\langle c_+ \rangle$ and $\langle c_- \rangle$ must then decrease with the increase of the ionic size because Eq. (19) is valid for both point and finite size ions. Therefore, a first consequence of the pressure increase is the increase of the coion exclusion with the ion size, which has an important effect on the CE, as explained below. The increase of the pressure also leads to a decrease of the counterion concentration close to the pore wall respect to the point ions case. Note that the pressure increase has no effect on the ions if their size is negligible. These effects are shown in Fig. 2.

The electric potential gradient at $r = a^*$, determined by the boundary condition of Eq. (12), increases with the ionic size. Therefore, $|\mathrm{d}\psi/\mathrm{d}r|$ increases with the ion size and so does the electric potential as shown in Fig. 3. Note also that, since ionic concentrations are exponential functions of the electrical potential (see

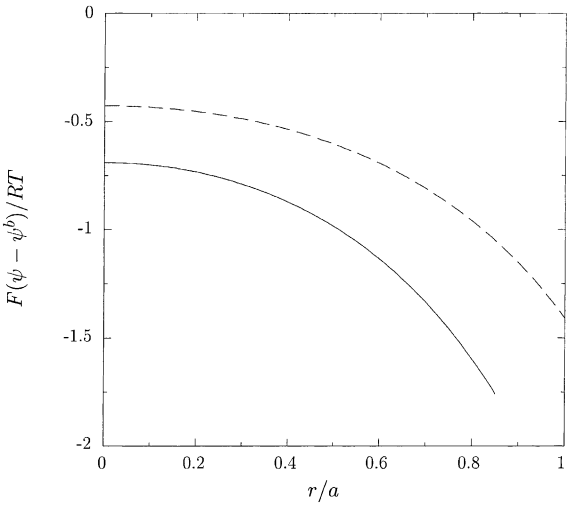

Fig. 3. Electric potential profile (normalized to the thermal potential RT/F) inside the pore for $a_i/a = 0.15$ and $c^{\text{b}}/X = 0.5$. Solid and dashed lines represent finite size and point ions, respectively. Note that for finite size ions, the upper limit of the radial variable is $a^* = a - a_i = 0.85a$.

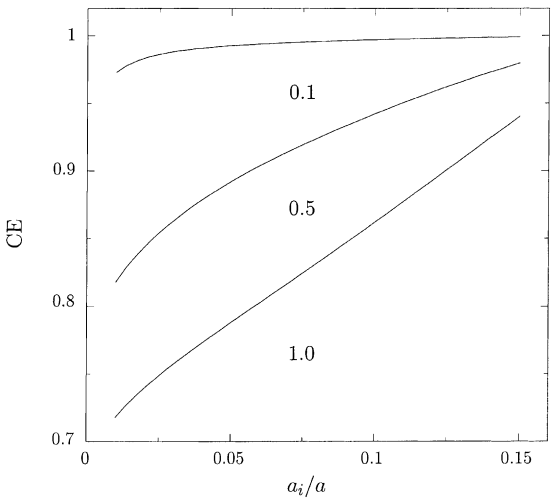

Fig. 4. CE as a function of a_i/a for different values of c^b/X (shown below the curves).

Eq. (15)), small changes in the potential profile near the pore surface may lead to significant changes in the concentrations close to this surface.

Fig. 4 shows the dependence of the CE with a_i/a for different values of c^b/X. Since the ionic radius has been fixed to $a_i = 0.2$ nm, the variation of a_i/a corresponds to changes in the pore radius. In particular, the values $a_i/a = 0.05$, 0.10, and 0.15 correspond to $a =$ 4.0, 2.0, and 1.3 nm, respectively. The curves in Fig. 4 clearly indicate that the CE increases with decreasing pore radius. Similarly, calculations carried out keeping constant the pore radius and varying the ionic radius show that the CE increases with increasing ionic size. In order to explain this trend, it is convenient to relate the CE to the average ionic concentrations. For the sake of simplicity, consider that convection is negligible and integrate Eq. (6) over the pore cross-section to obtain

$$J_i \approx -z_i D_i \frac{F}{RT}\frac{\mathrm{d}V}{\mathrm{d}x}\pi(a_i^*)^2\langle c_i\rangle, \tag{24}$$

where $\pi(a_i^*)^2$ is the area of the pore section available for the ions. Introducing Eq. (24) into Eq. (1) yields the simple relation

$$\mathrm{CE} \approx \frac{\langle c_+\rangle}{\langle c_+\rangle + \langle c_-\rangle}, \tag{25}$$

which becomes exact in the absence of convection. Recalling that X is defined as $\langle c_+\rangle - \langle c_-\rangle$ whose value is fixed by Eq. (19), we can transform Eq. (25) to

$$\mathrm{CE} \approx 1 - \frac{\langle c_-\rangle}{2\langle c_-\rangle + X}. \tag{26}$$

The dependence of the CE with a_i/a observed in Fig. 4 can now be qualitatively explained with the help of Fig. 2. One of the main implications of finite ion size is a larger coion exclusion, i.e. a decrease of $\langle c_-\rangle$ with increasing a_i/a. Therefore, Eq. (26) shows that the CE increases with increasing a_i/a.

The effect of the ratio c^b/X on the CE in Fig. 4 can also be explained by simple arguments. In the low external concentration limit, the average concentration of point coions is approximately given by $\langle c_-^0\rangle \approx (c^b)^2/X$ [24,26,27]. Thus, Eq. (26) reduces to

$$\mathrm{CE} \approx \mathrm{CE}^0 \approx \frac{1 + (c^b/X)^2}{1 + 2(c^b/X)^2}. \tag{27}$$

Eq. (27) yields the values 0.67, 0.83, and 0.99 for $c^b/X = 1.0$, 0.5, and 0.1, respectively, which is in agreement with the results shown in Fig. 4 for $a_i/a \ll 1$, the limit when the approximation $\langle c_-\rangle \approx \langle c_-^0\rangle \approx (c^b)^2/X$ is valid.

Eqs. (24)–(27) allow for simple estimations of the CE in the absence of convection, but convection is present both in real experiments and in the calculations presented in Fig. 4. Therefore, it is interesting to analyze the effect of convection on the CE. To this end, we have also carried out calculations of the CE imposing zero convective flow (i.e. neglecting the last term in Eq. (3)). Fig. 5 shows the behavior of the CE as a function c^b/X in the presence (a) and in the absence (b) of convection for the size ratios $a_i/a = 0.05$, 0.10, and 0.15. To compare the relative importance of convection and finite ion size, similar figures have also been prepared for the case of point ions. The dashed lines in Fig. 5(c) and (d) have been calculated for the pore radii $a = 4.0$, 2.0, and 1.3 nm, the same values as in Fig. 5(a) and (b). The first conclusion drawn from these figures is that the effect of convection on the CE is of the same order than that attributed to ionic size. For instance, the decrease of the CE when convection is neglected amounts to 13% when $a_i/a = 0.1$ and $c^b/X = 1.0$ (compare Fig. 5(a) with (b)), while the decrease of the CE due to ionic size amounts to 7% when convection has been accounted for (compare Fig. 5(a) with the curve for $a = 2.0$ nm of Fig. 5(c)).

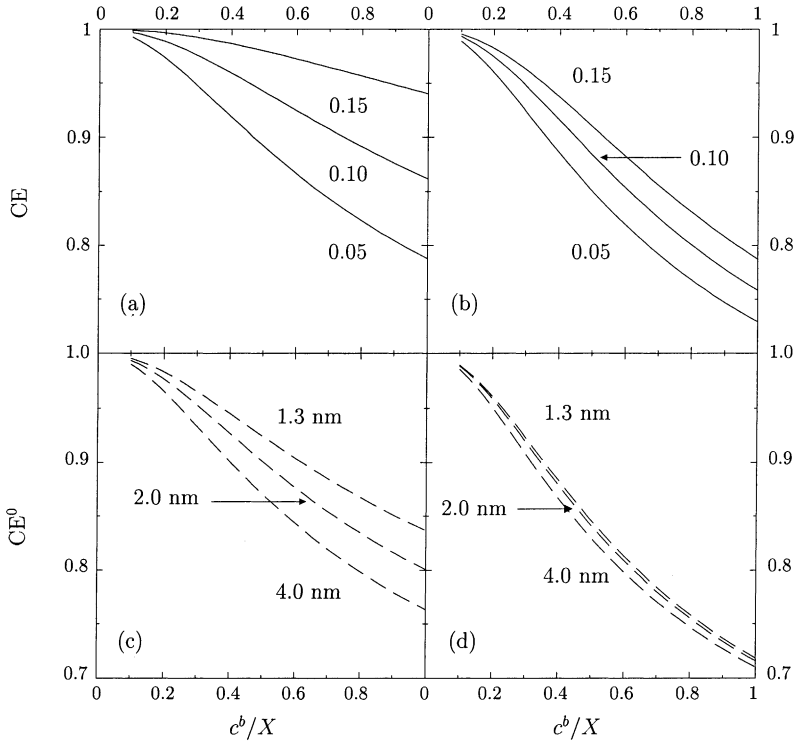

Fig. 5. CE as a function of c^b/X for finite size (continuous lines) and point (dashed lines) ions when convection is either considered ((a) and (c)) or neglected ((b) and (d)). The values have been calculated for the a_i/a ratios shown in the figures in the finite size ion case. When a_i/a ratios are 1.3, 2.0, and 4.0 nm. These pore radii are used in the calculations for point ions ((c) and (d)).

Keeping the convective term in Eq. (6) and averaging over the pore section, Eq. (25) can be generalized to

$$\mathrm{CE} \approx \frac{\langle c_+\rangle + \langle wc_+\rangle}{\langle c_+\rangle + \langle c_-\rangle + \langle wc_+\rangle - \langle wc_-\rangle}, \tag{28}$$

where w is defined as

$$w \equiv -\frac{u}{D_i(F/RT)(\mathrm{d}V/\mathrm{d}x)} > 0. \tag{29}$$

Eq. (29) is the ratio of convective to migrational flow for counterions. Since the potential distribution of Fig. 3 satisfies $F[\psi(r) - \psi(0)] \lesssim RT$, Eq. (28) can be approximated by

$$\mathrm{CE} \approx \frac{\langle c_+\rangle + \langle w\rangle\langle c_+\rangle}{\langle c_+\rangle + \langle c_-\rangle + \langle w\rangle X} = 1 - \frac{\langle c_-\rangle(1 - \langle w\rangle)}{2\langle c_-\rangle + X(1 + \langle w\rangle)}, \tag{30}$$

which is a generalization of Eq. (26). Since $\langle c_+\rangle \gtrsim X$, Eq. (30) requires that the CE increases with increasing convection, in agreement with the results of Fig. 5. This can also be understood considering that convection opposes migration in the coion flow case. On the contrary, the convective and migrational contributions to counterion flow are both in the same direction ($w > 0$). Hence, convection must increase the CE $= |J_+|/(|J_+| + |J_-|)$.

Finally, it is interesting to compare the effect of convection on the CE in the case of finite ion size (Fig. 5(a) and (b)) and point ions (Fig. 5(c) and (d)). The effect of convection is somehow larger in the case of finite size ions (compare, e.g. the CE values 0.94 and 0.79 for $a_i/a = 0.15$ and $c^b/X = 1.0$ in Fig. 5(a) and (b) with the CE values 0.84 and 0.72 for $a = 1.3$ nm and $c^b/X = 1.0$ in Fig. 5(c) and (d)). This is attributed to the fact that ion size influences not only the ionic concentration and electric potential,

but also the solution velocity. When $c^b/X \ll 1$, there are practically no coions in the membrane solution, and hence, CE ≈ 1 irrespective of convection. However, when $c^b/X = 1.0$ there is a large amount of coions in the membrane, and the fact that convection opposes migration for coions (thus decreasing $|J_-|$) has a large influence on the CE. Since the convective velocity under these conditions is larger for finite size ions than for point ions, the change in the CE due to convection is larger for finite size ions than for point ions, as observed from Fig. 5(a)–(d).

4. Conclusions

The CE of a fixed charge membrane with narrow pores has been studied theoretically as a function of two relevant experimental parameters, a_i/a and c^b/X. The ratio of the CE values corresponding to the point and finite size ions has also been analyzed as a function of the above two parameters. It has been shown that a higher coion exclusion from the membrane (and then a higher CE) is obtained for finite size ions. The results have illustrated clearly that ion size effects can be significant for ionic transport through narrow charged pores when $a_i/a \approx 0.1$, as it is the case of ionic drug transport through paracellular pathways.

Acknowledgements

Financial support from the DGICYT (Ministry of Education of Spain) under Project no. PB98-0419 is gratefully acknowledged.

References

[1] W. Olivares, T.L. Croxton, D.A. McQuarrie, Electrokinetic flow in a narrow cylindrical capillary, J. Phys. Chem. 84 (1980) 867.
[2] G.B. Westermann-Clark, J.L. Anderson, Experimental verification of the space–charge model for electrokinetics in charged microporous membranes, J. Electrochem. Soc. 130 (1983) 839.
[3] M. Eigen, E. Wicke, Zur theorie der starken electrolyte, Naturwissenschaften 38 (1951) 453.
[4] E. Wicke, M. Eigen, Über den Einfluß des Raumbedarfs von Ionen in wäßriger Lösung auf ihre Verteilung im elektrischen Feld und ihre Aktivitäkoeffizienten, Z. Elektrochem. 56 (1952) 551.
[5] E. Wicke, M. Eigen, Raumbedarf und Aktivitätkoeffizienten starker Elektrolyte in wäßriger Lösung, Z. Naturforsch. 8a (1953) 161.
[6] E. Wicke, M. Eigen, The thermodynamics of electrolytes at higher concentration, J. Phys. Chem. 58 (1954) 702.
[7] V. Freise, Zur theorie der diffusen Doppelschicht, Z. Elektrochem. 56 (1952) 822.
[8] P.N. Pintauro, M.W. Verbrugge, The electric-potential profile in ion-exchange membrane pores, J. Membr. Sci. 44 (1989) 197.
[9] A.G. Guzman-García, P.N. Pintauro, M.W. Verbrugge, R.F. Hill, Development of a space charge transport model for ion exchange membranes, AIChE J. 36 (1990) 1061.
[10] S. Basu, M. Sharma, An improved space-charge model for flow through charged microporous membranes, J. Membr. Sci. 124 (1997) 77.
[11] I. Borukhov, D. Andelman, H. Orland, Steric effects in electrolytes: a modified Poisson–Boltzmann equation, Phys. Rev. Lett. 79 (1997) 435.
[12] V.N. Paunov, B.P. Binks, Analytical expression for the electrostatic disjoining pressure taking into account the excluded volume of the hydrated ions between charged interfaces in electrolyte, Langmuir 15 (1999) 2015.
[13] V.N. Paunov, R.I. Dimova, P.A. Kralchevsky, G. Broze, A. Mehreteab, The hydration repulsion between charged surfaces as an interplay of volume exclusion and dielectric saturation effects, J. Colloid Interface Sci. 182 (1996) 239.
[14] V. Pade, S. Stavchansky, Estimation of the relative contribution of the transcellular and paracellular pathway to the transport of passively absorbed drugs in the Caco—2 cell culture model, Pharm. Res. 14 (1997) 1210.
[15] A. Adson, T.J. Raub, P.S. Burton, C.L. Barsuhn, A.R. Hilgers, K.L. Audus, N.F.H. Ho, Quantitative approaches to delineate paracellular diffusion in cultured epithelial cell monolayers, J. Pharm. Sci. 83 (1994) 1529.
[16] W.H. Koh, H.P. Silverman, Anion transport in thin-channel cation exchange membranes, J. Membr. Sci. 13 (1983) 279.
[17] S. Koter, Influence of the layer fixed charge distribution on the performance of an ion-exchange membrane, J. Membr. Sci. 108 (1995) 177.
[18] A.E. Cárdenas, R.D. Coalson, M.G. Kurnikova, Test of continuum theories as models of ion channels. I. Poisson–Boltzmann theory versus Brownian dynamics, Biophys. J. 78 (2000) 2349.
[19] H. Reiss, I.C. Bassignana, Critique of the mechanism of superselectivity in ion exchange membranes, J. Membr. Sci. 11 (1982) 219.
[20] J.A. Manzanares, S. Mafé, J. Pellicer, Current efficiency enhancement in membranes with macroscopic inhomogeneities in the fixed charge distribution, J. Chem. Soc., Faraday Trans. 88 (1992) 2355.
[21] F.M.H. Villars, G.B. Benedek, Physics: with illustrative examples for medicine and biology, Vol. 2, Addison-Wesley, Cambridge, 1974.

[22] R.P. Buck, Kinetics of bulk and interfacial ionic motion: microscopic basis and limits for the Nernst–Planck equations applied to membranes systems, J. Membr. Sci. 17 (1984) 1.
[23] W.Y. Lo, K. Chan, Poisson–Boltzmann calculations of ions in charged capillaries, J. Chem. Phys. 101 (1994) 1431.
[24] N. Lakshminarayanaiah, Equations of Membrane Biophysics, Academic Press, New York, 1984.
[25] W.H. Press, B.P. Flannery, S.A. Teukolsky, W.T. Vetterling, Numerical Recipes in C, Cambridge University Press, Cambridge, 1988.
[26] R. Schlögl, U. Schödel, Über das Verhalten geladener Porenmembranen bei Stromdurchgang, Z. Phys. Chem. 5 (1955) 372.
[27] F. Helfferich, Ion Exchange, Dover, New York, 1995 .